Published in final edited form as:
Exp Neurol. 2012 May ; 235(1): 246–255. doi:10.1016/j.expneurol.2012.02.002.

Decreased expression of the glial water channel aquaporin-4 in the intrahippocampal kainic acid model of epileptogenesis

Darrin J. Lee[1], **Mike S. Hsu**[2], **Marcus M. Seldin**[3], **Janetta L. Arellano**[4], and **Devin K. Binder**[2]

[1]Department of Neurological Surgery, University of California, Davis, CA

[2]Center for Glial-Neuronal Interactions, Division of Biomedical Sciences, University of California, Riverside, CA

[3]Department of Physiology, Johns Hopkins University, Baltimore, MD

[4]University of California, Irvine, CA

Abstract

Recent evidence suggests that astrocytes may be a potential new target for the treatment of epilepsy. The glial water channel aquaporin-4 (AQP4) is expressed in astrocytes, and along with the inwardly-rectifying K^+ channel $K_{ir}4.1$ is thought to underlie the reuptake of H_2O and K^+ into glial cells during neural activity. Previous studies have demonstrated increased seizure duration and slowed potassium kinetics in $AQP4^{-/-}$ mice, and redistribution of AQP4 in hippocampal specimens from patients with chronic epilepsy. However, the regulation and role of AQP4 during epileptogenesis remain to be defined. In this study, we examined the expression of AQP4 and other glial molecules (GFAP, $K_{ir}4.1$, glutamine synthetase) in the intrahippocampal kainic acid (KA) model of epilepsy and compared behavioral and histologic outcomes in wild-type mice *vs.* $AQP4^{-/-}$ mice. Marked and prolonged reduction in AQP4 immunoreactivity on both astrocytic fine processes and endfeet was observed following KA status epilepticus in multiple hippocampal layers. In addition, $AQP4^{-/-}$ mice had more spontaneous recurrent seizures than wild-type mice during the first week after KA SE as assessed by chronic video-EEG monitoring and blinded EEG analysis. While both genotypes exhibited similar reactive astrocytic changes, granule cell dispersion and CA1 pyramidal neuron loss, there were an increased number of fluorojade-positive cells early after KA SE in $AQP4^{-/-}$ mice. These results indicate a marked reduction of AQP4 following KA SE and suggest that dysregulation of water and potassium homeostasis occurs during early epileptogenesis. Restoration of astrocytic water and ion homeostasis may represent a novel therapeutic strategy.

Keywords

seizure; status epilepticus; aquaporin; glial; mouse

Address correspondence to: Devin K. Binder, M.D., Ph.D., Center for Glial-Neuronal Interactions, Division of Biomedical Sciences, 1247 Webber Hall, University of California, Riverside, Riverside, CA 92521-0121, Tel: (951) 827-2224, Fax: (951) 827-5504, dbinder@ucr.edu.

Introduction

Recent evidence suggests that glial cells may play a role in epilepsy (Binder and Steinhäuser, 2006). First, many studies now link glial cells to modulation of synaptic transmission (Halassa and Haydon, 2010, Volterra and Meldolesi, 2005). Second, functional alterations of specific glial membrane channels and receptors have been discovered in epileptic tissue (Seifert, et al., 2006, Steinhäuser and Seifert, 2002). Third, direct stimulation of astrocytes has been shown to be sufficient for neuronal synchronization in epilepsy models (Tian, et al., 2005).

The aquaporins (AQPs) are a family of membrane protein water channels expressed in many cell types and tissues that facilitate bi-directional water transport in response to osmotic gradients (Verkman, 2002, Verkman, 2005). Aquaporin-4 (AQP4) is expressed by glial cells, especially at specialized membrane domains including astroglial endfeet in contact with blood vessels and astrocyte membranes that ensheathe glutamatergic synapses (Nagelhus, et al., 2004, Nielsen, et al., 1997).

Modulation of water and potassium homeostasis by AQP4 could dramatically affect seizure susceptibility. Brain tissue excitability is exquisitely sensitive to osmolarity and the size of the extracellular space (ECS) (Schwartzkroin, et al., 1998). Decreasing ECS volume produces hyperexcitability and enhanced epileptiform activity (Dudek, et al., 1990, Roper, et al., 1992); conversely, increasing ECS volume with hyperosmolar medium attenuates epileptiform activity (Dudek, et al., 1990, Traynelis and Dingledine, 1989). These experimental data parallel extensive clinical experience indicating that hypo-osmolar states lower seizure threshold while hyperosmolar states elevate seizure threshold (Andrew, et al., 1989). Second, millimolar and even submillimolar increases in extracellular potassium concentration powerfully enhance epileptiform activity in the hippocampus (Feng and Durand, 2006, Traynelis and Dingledine, 1988).

Emerging work indeed demonstrates dysregulation of water and potassium homeostasis in patients with mesial temporal lobe epilepsy (Binder and Steinhäuser, 2006). Imaging studies demonstrate abnormal T2 prolongation by MRI in the epileptic hippocampus, thought to be due to increased water content (Mitchell, et al., 1999) accompanied by alterations in apparent diffusion coefficient (ADC) (Hugg, et al., 1999). The expression and subcellular localization of AQP4 have been shown to be altered in sclerotic hippocampi obtained from patients with MTS (Lee, et al., 2004), in particular a reduction in perivascular membrane expression (Eid, et al., 2005).

We recently demonstrated that AQP4$^{-/-}$ mice have significantly prolonged seizure duration associated with a deficit in extracellular K^+ clearance (Binder, et al., 2006). This result together with the alterations in AQP4 seen in human tissue specimens suggest a possible pro-epileptogenic role of AQP4 dysregulation (Dudek and Rogawski, 2005, Hsu, et al., 2007, Wetherington, et al., 2008). However, the timing, mechanisms, and role of AQP4 regulation during epileptogenesis remain unknown.

In this study, we used the well-defined intrahippocampal kainic acid model (Arabadzisz, et al., 2005, Bouilleret, et al., 1999, Riban, et al., 2002) to examine the regulation of AQP4 and other glial molecules (GFAP, $K_{ir}4.1$, glutamine synthetase) during epileptogenesis. In addition, using chronic video-EEG recording, we quantified and compared frequency of spontaneous recurrent seizures (SRS) between wild-type and AQP4$^{-/-}$ mice. Finally, we compared histological alterations and cell death in wild-type vs. AQP4$^{-/-}$ mice.

Materials and Methods

All experiments were conducted in accordance to the guidelines set forth by the National Institutes of Health and were approved by the University of California, Irvine Institutional Animal Care and Use Committee (IACUC). Animals were housed under controlled conditions (12hr light/12hr dark), and food and water were provided to the mice *ad libitum*.

Animals and surgery

Adult (6–8 week-old) $AQP4^{+/+}$ and $AQP4^{-/-}$ litter-matched male mice were used. The $AQP4^{-/-}$ mice were generated as previously described (Ma, et al., 1997). Mice were anesthetized with an intraperitoneal injection of a mixture of ketamine/xylazine (ketamine 80 mg/kg, xylazine 10 mg/kg), mounted on a stereotaxic frame (Stoelting, Wood Dale, IL) and skin incision was made to expose the skull. Stereotaxic coordinates of the hippocampus were identified (Paxinos and Franklin, 2001) and a 0.6 mm burr hole was made (AP = −1.8 mm, ML = +1.6 mm) using a 45,000 rpm high speed drill (Drummond Scientific, Broomall, PA). Mice were stereotaxically injected using a microinjector (Nanoject, Drummond Scientific, Broomall, PA) with either 100 nl of a 20-mM solution of kainic acid or 100 nl of 0.9% saline (control mice) into the right dorsal hippocampus (AP = −1.8 mm, ML = +1.6 mm, DV = 1.9 mm (Arabadzisz, et al., 2005)). Bipolar stainless steel wire electrodes were then implanted into the right dorsal hippocampus (AP = −1.8 mm, ML = +1.6 mm, DV = 2.0 mm). Bipolar electrodes were made by twisting two stainless steel wires (California Fine Wire, Grover Beach, CA) and soldering on pin connectors (Newark, Chicago, IL) to the ends. Monopolar ground electrodes were implanted anterior to bregma. Electrodes were secured to the skull with polymethylmethacrylate dental acrylic.

Video-EEG monitoring

Animals were freely moving and continuously monitored 24 hours per day up to 14 days using a digital video camera (Sony HDR-HC5, Sony Electronics, San Diego, CA). EEGs were continuously recorded with a digital acquisition system (MP150 with EEG100C amplifiers, Biopac Systems Inc., Santa Barbara, CA).

EEG analysis

Only mice that experienced status epilepticus (SE) were evaluated in this study. SE was defined as continuous tonic-clonic seizure activity for at least 3 hours. Spontaneous seizures during the post-SE period of epileptogenesis were defined as spiking epileptiform burst activity lasting for at least 5 seconds at a frequency of ≥3 Hz. Seizure analysis was performed blinded to genotype and motion artifacts were excluded from analysis.

Immunohistochemistry

Histological analysis was performed on control ($AQP4^{+/+}$ and $AQP4^{-/-}$) and experimental ($AQP4^{+/+}$ and $AQP4^{-/-}$) mice at 1 day, 4 days, 7 days, 14 days and 30 days after SE. Mice were deeply anesthetized with an intraperitoneal injection of sodium pentobarbital (200 mg/kg) and perfused transcardially with ice-cold phosphate-buffered saline (PBS; pH 7.4) followed by 4% paraformaldehyde, pH 7.4. Brains were postfixed overnight in 4% paraformaldehyde at 4°C followed by cryoprotection in 30% sucrose in PBS at 4°C. Coronal 50 μm thick sections were cut from frozen blocks with a cryostat (Leica 1900, Leica Microsystems, Bannockburn, IL). Sections were stored in PBS at 4°C. Sections were blocked with 5% normal goat serum in 0.1 M PBS, then incubated with primary antibody to AQP4 (1:200; Millipore, Temecula, CA), GFAP (1:100; Millipore, Temecula, CA), neuronal-specific nuclear protein (NeuN; 1:100; Millipore, Temecula, CA), $K_{ir}4.1$ (1:100, Alomone, Jerusalem, Israel), and/or glutamine synthetase (1:100; Santa Cruz Biotechnology,

Santa Cruz, CA) in 0.3% Triton X-100 at 4°C overnight. After rinsing with PBS, sections were incubated with a species-specific secondary antibody conjugated with Alexa 488, 594, 647 or a TSA kit (Molecular Probes/Invitrogen, Carlsbad, CA) for visualization and then mounted in Vectorshield (Vector Laboratories, Burlingame, CA). Images were obtained on a fluorescence microscope (BX51; Olympus, San Diego, CA). Images and analysis of sections presented are of the hemisphere contralateral to the side of injection, except where otherwise noted (NeuN).

Quantification of immunoreactivity

Quantitative analysis of staining intensity was performed using densitometry. FIuorescent images of the immunoreactivity of various stains within the hippocampus were captured and analyzed using Slidebook (Intelligent Imaging Innovations, Inc, Santa Monica, CA). A square box delineating the region of interest with the width of the pyramidal cell layer of the hippocampus was placed in each of the layers of the hippocampus; stratum oriens (SO), stratum pyramidale (SP), stratum radiatum (SR), stratum lacunosum moleculare (SLM), dentate gyrus molecular layer (ML), dentate gyrus granule cell layer (GC), and hilus of the dentate gyrus (DG). Intensity per unit area was calculated and analyzed.

Fluoro-jade B histochemistry

Neuronal degeneration was characterized using fluoro-jade B (FJ-B) staining as described (Schmued, et al., 1997). Sections were mounted onto slides, dehydrated, immersed in a solution containing 1% sodium hydroxide in 80% ethanol, rehydrated in 70% alcohol, rinsed with PBS, transferred to a solution of 0.06% potassium permanganate and blocked for 30 minutes with agitation. Following the blocking process, slides were then washed with PBS to remove excess potassium permanganate. The staining solution was prepared by diluting a stock solution of 0.1% stock solution of FJ-B (Histo-Chem Inc., Jefferson, AR) 1:10 in 0.1% acetic acid solution. Slides were allowed to incubate at room temperature for 30 minutes in the 0.01%FJ-B/0.1% acetic acid solution. After the incubation, sections were washed 2–3 times with PBS and once with distilled water. Sections were left to dry overnight prior to imaging. Images of each section were captured using a fluorescent microscope (BX51; Olympus, San Diego, CA) and the number of FJ-B-positive cells in the hippocampus was counted.

Results

Seizure analysis

After injection of intra-hippocampal kainic acid, status epilepticus was induced in both $AQP4^{+/+}$ and $AQP4^{-/-}$ mice as evidenced electrographically (Figure 1A) and behaviorally (data not shown). Spontaneous seizures developed during post-status epilepticus (SE) days 2–11 (3.0 ± 0.9 days) in $AQP4^{+/+}$ animals and post-SE days 2–3 (2.1 ± 0.1 days) in $AQP4^{-/-}$ animals (Figures 1B, 1C, respectively). While spontaneous seizures developed in all experimental animals, $AQP4^{-/-}$ mice exhibited more seizures during the first week after injection (early epileptogenic period, Figure 2). Specifically, $AQP4^{-/-}$ mice had a higher mean # of seizures per day during post-SE days 1–7 than $AQP4^{+/+}$ mice (14.8±2.1 vs. 6.5±1.1, respectively; $p<0.05$, 2-way RM ANOVA) and a greater number of seizures overall during the first 7 days (103.5±23.8 vs. 45.5±14.0, respectively; $p<0.05$, t-test). In addition, there was a trend toward greater total seizure duration per day between $AQP4^{-/-}$ mice (282.8 ± 41.2 sec) and $AQP4^{+/+}$ mice (178.6 ± 28.0 sec) but this did not reach statistical significance ($p>0.05$). After post-SE day 7 through the end of the recording period (day 14), there were no significant differences in frequency or seizure duration between genotypes. No animals that were injected with saline developed status epilepticus or spontaneous seizures.

In order to verify that seizures propagated to the contralateral hippocampus in the epileptogenic period, a subset of mice (n=4) were implanted with bilateral hippocampal electrodes. These experiments confirmed that, similar to previous results (Arabadzisz, et al., 2005), following unilateral KA injection seizures occurred in both hippocampi (Supplemental Figure 1). There were fewer seizures in the hippocampus contralateral to the injection in both $AQP4^{+/+}$ and $AQP4^{-/-}$ mice (data not shown).

AQP4 immunoreactivity

In this group of studies, we used a sensitive and specific AQP4 immunohistochemical protocol that has been previously validated in detail using $AQP4^{-/-}$ tissue (Hsu, et al., 2011). No specific immunoreactivity was observed in the absence of anti-AQP4 primary antibody. Compared to saline controls, AQP4 immunoreactivity was significantly decreased on post-SE day 1 (saline control: 730.9 ± 59.5 vs. post-SE day 1: 406.2 ± 25.8 ADU/mm^2, $p<0.05$). This initial decrease was followed by a slow return to near-normal levels over the next 30 days (Figure 3A). Saline controls did not demonstrate any significant differences in AQP4 levels at any time point (data not shown). When analyzing the hippocampal layers individually, there were additional significant differences in various hippocampal layers and time points (Figure 3B-H) relative to control. Specifically, there were no significant differences between saline control and experimental animals in stratum oriens at any time point. Relative to saline controls, stratum pyramidale demonstrated decrease at post-SE day 1 (969.3±137.4 vs. 463.1±25.1, respectively; $p<0.05$) and post-SE day 4 (969.3±137.4 vs. 498.2±30.7, respectively; $p<0.05$). Stratum radiatum demonstrated decrease at post-SE day 1 (394.2±34.5 vs. 1248.9±205.0, $p<0.05$), post-SE day 4 (428.3±35.7 vs. 1248.9±205.0, $p<0.05$) and post-SE day 7 (738.3±76.4 vs. 1248.9±205.0, $p<0.05$). The dentate granule cell layer demonstrated AQP4 decrease at all time points except for post-SE day 14. Decreased AQP4 immunoreactivity was noted at all time points post-SE in stratum lacunosum moleculare, the molecular layer and the hilus of the dentate gyrus (Figure 3B-H).

GFAP immunoreactivity

In both $AQP4^{+/+}$ and $AQP4^{-/-}$ animals, marked increases in GFAP immunoreactivity were detected on post-SE days 4, 7, and 14 in all layers of the hippocampus, followed by a slight decrease at post-SE day 30 (Figure 4). No significant differences were observed in GFAP immunoreactivity between $AQP4^{+/+}$ (Figure 5A, 5C) and $AQP4^{-/-}$ (Figure 4B, 4D) mice; in both genotypes, astrocyte morphology became reactive with ramified with thickened processes (Figure 4,5).

K_{ir}4.1 immunoreactivity

Overall K_{ir}4.1 immunoreactivity in post-SE animals did not differ significantly from control $AQP4^{+/+}$ mice (Figure 6A). In addition, there were also no significant differences in overall Kir4.1 levels between post-SE $AQP4^{+/+}$ and post-SE $AQP4^{-/-}$ mice for all time points in this study (data not shown). However, significant focal K_{ir}4.1 immunoreactivity was detected on reactive astrocytes of CA1 stratum radiatum and stratum lacunosum moleculare on post-SE days 4 and 7 (Figure 6A, Supplemental Figure 2B). Reactive astrocytes exhibited an upregulation of K_{ir}4.1 and GFAP expression as well as thicker processes (Figure 5).

Glutamine synthetase (GS) immunoreactivity

A modest but statistically significant increase in GS immunoreactivity was observed at post-SE days 4 and 7 in $AQP4^{+/+}$ mice when compared to saline controls (Figure 6B). No significant differences were seen at longer time points (14 and 30 days post-SE). In addition, as for K_{ir}4.1, there were no significant differences in GS immunoreactivity between $AQP4^{-/-}$ and $AQP4^{+/+}$ mice (data not shown).

NeuN immunoreactivity

After KA-induced SE, a dispersion of the cells of the granule cell layer of the dentate gyrus was noted in both $AQP4^{+/+}$ and $AQP4^{-/-}$ mice (Figure 7). The dispersion occurred only in the hippocampus ipsilateral to the injection. Significant progressive loss of CA1 pyramidal cell layer NeuN immunoreactivity was observed, greatest at post-SE day 30 (Figure 7).

Fluoro-jade B histochemistry

From post-SE day 1 to post-SE day 14, sections from both genotypes exhibited FJ-B-positive cells. These cells were mostly observed in CA3 and hilus of the dentate gyrus in the hippocampus ipsilateral to the injection (Figure 8). Following blinded analysis, there were significantly more FJ-B-positive cells in the $AQP4^{-/-}$ mice relative to $AQP4^{+/+}$ mice on post-SE day 1 (173.1±33.4 vs. 54.6±30.8, $p<0.05$) and post-SE day 4 (94.0±18.6 vs. 40.4±9.0, $p<0.05$) (Figure 8B). Fewer FJ-B-positive cells and no significant genotypic differences were observed at longer time points (Figure 8B).

Discussion

In this study, we have used the intrahippocampal kainic acid model to examine changes in glial cell molecules early during the process of epileptogenesis. This led to several novel findings: first, $AQP4^{-/-}$ mice had more spontaneous recurrent seizures than wild-type mice during the first week after SE; second, there is a dramatic and prolonged downregulation of AQP4 immunoreactivity in the hippocampus following KA SE; third, while both genotypes exhibited similar reactive astrocytic changes, granule cell dispersion and CA1 pyramidal neuron loss, $AQP4^{-/-}$ mice had an increased number of fluoro-jade positive cells early after KA SE. These results support the hypothesis that intense seizures regulate AQP4 expression and may lead to a functionally relevant dysregulation of water and potassium homeostasis during epileptogenesis.

Increased seizure frequency in $AQP4^{-/-}$ mice

Previous results in acute seizure models demonstrated that $AQP4^{-/-}$ mice have a higher seizure threshold (Binder, et al., 2004, Binder, et al., 2006) but that seizures once elicited demonstrated a prolonged duration, presumably due in part to impaired K^+ reuptake (Binder, et al., 2006). Using chronic video-EEG recording for the first two weeks after KA SE, we did not find a statistically significant difference in total seizure duration between $AQP4^{+/+}$ and $AQP4^{-/-}$ mice in the intrahippocampal KA model, but rather found an increase in the frequency of seizures in the $AQP4^{-/-}$ animals during the first week after KA SE (Figure 2). Of course, in this chronic model of epileptogenesis, the initiation of SRS depends on multiple factors. For example, recent studies have indicated that following KA SE, reactive astrocytes exhibit alterations in glutamate transporter-dependent currents and also substantially increased dye coupling (Takahashi, et al., 2010), although interestingly this group did not observe a change in astrocyte K+ currents early after SE. Impaired K^+ reuptake in the $AQP4^{-/-}$ mice as previously described (Binder, et al., 2006) would presumably lead to an increased excitability at least during the early phase of epileptogenesis which is consistent with the increased seizure frequency observed. Our novel finding of slightly increased cell death at 1 and 4 days following SE in the $AQP4^{-/-}$ mice (Figure 8) may also contribute to an increased excitability after SE. Interestingly, since there is downregulation of AQP4 in the wild-type mice during this period, the wild-type mice may thus develop a “functional knockdown” of AQP4 and this may limit difference between the genotypes thereafter. Acquired dysregulation of AQP4 could lead to hyperexcitability by both astrocyte swelling-induced ephaptic interactions and impaired K^+ homeostasis (Hsu, et al., 2007, Wetherington, et al., 2008).

Decrease in AQP4 immunoreactivity following status epilepticus

In studies in human patients with mesial temporal sclerosis (MTS), it was noted that hippocampal tissue sections have increased AQP4 expression (Lee, et al., 2004). However, these studies were conducted in chronic epileptic tissue and not much is known about the expression of AQP4 during the development of epilepsy. Previous studies demonstrated alteration in the expression and subcellular localization of AQP4 in sclerotic hippocampi obtained from patients with MTS (Lee, et al., 2004), in particular a reduction in perivascular membrane expression (Eid, et al., 2005).

Here, using a validated AQP4 immunohistochemical protocol (Hsu, et al., 2011), we report a marked, immediate and prolonged decrease in AQP4 immunoreactivity following KA SE. Compared to controls, AQP4 immunoreactivity was decreased in stratum lacunosum moleculare, the molecular layer and the dentate gyrus for all the time points in this study, and in a number of other layers of the hippocampus in the initial days following SE. The loss of AQP4 immunoreactivity occurred on both the endfeet and fine processes of astrocytes throughout the hippocampal layers. The mechanism of this decrease remains unclear: AQP4 could be downregulated or internalized from the cell surface. Also, it is not clear whether AQP4 downregulation is due entirely to the initial episode of SE or whether SRS maintain AQP4 downregulation. Further studies would be required to determine whether brief or shorter seizures have the capacity to downregulate AQP4.

K_{ir}4.1 immunoreactivity following status epilepticus

The inwardly-rectifying potassium channel K_{ir}4.1 exhibits heterogenous expression throughout the brain (Poopalasundaram, et al., 2000), but is the predominant K_{ir} subtype within the hippocampus (Seifert, et al., 2009). K_{ir}4.1 is thought to contribute to K^+ reuptake and spatial K^+ buffering by glial cells (Newman, 1986, Newman, et al., 1984), and pharmacological or genetic inactivation of K_{ir}4.1 leads to impairment of extracellular K^+ regulation (Ballanyi, et al., 1987, Djukic, et al., 2007, Kofuji, et al., 2000, Kofuji and Newman, 2004, Neusch, et al., 2006). Dysfunction of astroglial K_{ir} channels has also been found in specimens from patients with temporal lobe epilepsy (Hinterkeuser, et al., 2000, Kivi, et al., 2000) and impaired K^+ uptake by astrocytes through K_{ir} channels may contribute to epileptogenesis in a mouse model of TSC (Jansen, et al., 2005).

Based on its demonstrated importance to K^+ homeostasis, we also examined K_{ir}4.1 immunoreactivity in the KA SE model. Interestingly, in contrast to AQP4, we did not observe downregulation of Kir4.1 at the time points studied. Rather, K_{ir}4.1 was observed upregulated specifically on reactive astrocytes, especially in CA1 SR and SLM (Figure 5B), on which AQP4 was absent (Figure 5A). Thus, there appears to be distinct regulation of AQP4 and K_{ir}4.1. While initial studies indicated a subcellular co-localization of AQP4 with K_{ir}4.1 in the retina (Connors, et al., 2004, Nagelhus, et al., 2004), more recent studies indicate a lack of interaction between the two proteins (Zhang and Verkman, 2008).

Changes in glutamine synthetase and GFAP immunoreactivity following SE

Glutamine synthetase (GS) catalyzes the conversion of glutamate to glutamine in astrocytes and has been found to be decreased in the sclerotic hippocampus of temporal lobe epilepsy patients (Eid, et al., 2004, van der Hel, et al., 2005). In our study, we observed a transient increase in GS immunoreactivity on post SE days 1 and 4 (Figure 6B, 6D). This is similar to that which was observed in rats during the latent period following initial seizure insult prior to the onset of spontaneous seizures (Hammer, et al., 2008). In that study, GS was increased in the latent phase compared with controls, as assessed by Western blots of whole hippocampal formation and subregions. Compared with the latent phase, the chronic phase revealed a lower level of hippocampal GS content (Hammer, et al., 2008). Studies in other

models have demonstrated that newly generated astrocytes after SE may have lower levels of GS (Kang, et al., 2006).

Like many previous studies, we observed upregulation of GFAP on reactive astrocytes following KA SE (Figure 6). No significant differences were observed in GFAP immunoreactivity between wild-type and AQP4$^{-/-}$ mice at any time point. The remarkable congruity of GFAP upregulation and similar morphology of reactive astrocytes regardless of genotype suggests that AQP4 does not directly affect astrocyte cytoskeletal reactivity and reactive astrocytosis. This is interesting in light of previous studies which demonstrated impaired migration of AQP4-deficient cells to the site of stab injury in cortex (Saadoun, et al., 2005). Taken together, these data indicate an effect of AQP4 on cell migration but not on cytoskeletal changes associated with glial scar formation.

Changes in neuronal histology in IH KA model

Previous studies in the IH KA model (Arabadzisz, et al., 2005, Bouilleret, et al., 1999, Riban, et al., 2002) demonstrated that the model reproduces morphological characteristics of mesial temporal sclerosis, including neuronal loss, gliosis, reorganization of neurotransmitter receptors, mossy fiber sprouting, and granule cell dispersion. We confirmed the pattern of neuronal loss in CA1 and progressive dentate granule cell dispersion as assessed by NeuN immunoreactivity and found that the pattern was not significantly different in AQP4$^{-/-}$ mice (Figure 7). Compared with previous papers, we contribute the finding that dentate granule cell dispersion occurs as early as 7 days after SE in this model (Figure 7). Granule cell dispersion is thought to be neurogenesis-independent (Nitta, et al., 2008) and caused by reelin deficiency (Haas, et al., 2002, Haas and Frotscher, 2010) and a recent study in the IH KA model demonstrates that it can be inhibited by hippocampal deafferentation (Pallud, et al., 2010).

Despite the overall lack of difference between genotypes in chronic histologic changes described above, FJ-B histochemistry demonstrated an increased number of degenerating cells in AQP4$^{-/-}$ mice on post-SE days 1 (Figure 8). The location of these cells was in the hilus (Figure 8), CA3 and CA1 regions (not shown). The mechanism of slightly increased cell death in AQP4$^{-/-}$ mice is unclear but again may relate to impaired K^+ and possibly glutamate homeostasis. Another possibility is that the actual KA SE was more intense or of longer duration in the AQP4$^{-/-}$ mice thus constituting a greater insult; however, great care was taken to observe and quantify the SE with video-EEG and no difference in duration or intensity of the initial SE were observed between genotypes. These data are the first to indicate a possible neuroprotective role of AQP4 aside from the well-known role of AQP4 in brain water balance (Manley, et al., 2004, Verkman, 2005).

Conclusion

Future studies will need to examine the mechanisms of AQP4 regulation in greater detail at mRNA and protein levels. In addition to previously described roles in K+ regulation, the lack of AQP4 also appears to promote hyperexcitability and neurotoxicity early after SE. Still undetermined is the contribution of astrocytic cell swelling itself to excitotoxicity and seizure generation. Since astrocytes release glutamate under hypoosmolar stress through a calcium-independent pathway (Fiacco, et al., 2007), swollen AQP4-deficient astrocytes could potentially contribute directly to excitability and excitotoxicity by increased release of glutamate, in addition to the more established contribution of loss of K^+ buffering. It will be interesting to elucidate the role of astrocytic swelling and astrocytic swelling-induced glutamate release in acute seizures and during epileptogenesis, as well as to develop novel methods to upregulate AQP4 as a possible therapy to restore water and potassium homeostasis.

Supplementary Material

Refer to Web version on PubMed Central for supplementary material.

Acknowledgments

This study was supported by a Mentored Clinical Scientist Research Career Development Award (NINDS K08 NS059674) (DKB), an American Epilepsy Society/Milken Family Foundation Early Career Physician-Scientist Award (DKB) and a Howard Hughes Medical Institute medical student research fellowship (DJL). The authors gratefully acknowledge Alan S. Verkman (UCSF) for the provision of the AQP4$^{-/-}$ mice.

Abbreviations

AQP4	aquaporin-4
FJ-B	fluoro-jade B
GS	glutamine synthetase
KA	kainic acid
MTS	mesial temporal sclerosis
SE	status epilepticus
SRS	spontaneous recurrent seizures

References

1. Amiry-Moghaddam M, Williamson A, Palomba M, Eid T, de Lanerolle NC, Nagelhus EA, Adams ME, Froehner SC, Agre P, Ottersen OP. Delayed K^+ clearance associated with aquaporin-4 mislocalization: phenotypic defects in brains of alpha-syntrophin-null mice. Proceedings of the National Academy of Sciences. 2003; 100:13615–13620.
2. Andrew RD, Fagan M, Ballyk BA, Rosen AS. Seizure susceptibility and the osmotic state. Brain Res. 1989; 498:175–180. [PubMed: 2790471]
3. Arabadzisz D, Antal K, Parpan F, Emri Z, Fritschy JM. Epileptogenesis and chronic seizures in a mouse model of temporal lobe epilepsy are associated with distinct EEG patterns and selective neurochemical alterations in the contralateral hippocampus. Experimental Neurology. 2005; 194:76–90. [PubMed: 15899245]
4. Ballanyi K, Grafe P, ten Bruggencate G. Ion activities and potassium uptake mechanisms of glial cells in guinea-pig olfactory cortex slices. J Physiol. 1987; 382:159–174. [PubMed: 2442359]
5. Binder DK, Oshio K, Ma T, Verkman AS, Manley GT. Increased seizure threshold in mice lacking aquaporin-4 water channels. Neuroreport. 2004; 15:259–262. [PubMed: 15076748]
6. Binder DK, Steinhäuser C. Functional changes in astroglial cells in epilepsy. Glia. 2006; 54:358–368. [PubMed: 16886201]
7. Binder DK, Yao X, Zador Z, Sick TJ, Verkman AS, Manley GT. Increased seizure duration and slowed potassium kinetics in mice lacking aquaporin-4 water channels. Glia. 2006; 53:631–636. [PubMed: 16470808]
8. Bouilleret V, Ridoux V, Depaulis A, Marescaux C, Nehlig A, Le Gal La Salle G. Recurrent seizures and hippocampal sclerosis following intrahippocampal kainate injection in adult mice: electroencephalography, histopathology and synaptic reorganization similar to mesial temporal lobe epilepsy. Neuroscience. 1999; 89:717–729. [PubMed: 10199607]
9. Connors NC, Adams ME, Froehner SC, Kofuji P. The potassium channel Kir4.1 associates with the dystrophin-glycoprotein complex via alpha-syntrophin in glia. J Biol Chem. 2004; 279:28387–28392. [PubMed: 15102837]
10. Djukic B, Casper KB, Philpot BD, Chin L-S, McCarthy KD. Conditional knock-out of Kir4.1 leads to glial membrane depolarization, inhibition of potassium and glutamate uptake, and enhanced short-term synaptic potentiation. J Neurosci. 2007; 27:11354–11365. [PubMed: 17942730]

11. Dudek FE, Obenhaus A, Tasker JG. Osmolality-induced changes in extracellular volume alter epileptiform bursts independent of chemical synapses in the rat: importance of non-synaptic mechanisms in hippocampal epileptogenesis. Neurosci Lett. 1990; 120:267–270. [PubMed: 2293114]
12. Dudek FE, Rogawski MA. Regulation of brain water: is there a role for aquaporins in epilepsy? Epilepsy Curr. 2005; 5:104–106. [PubMed: 16145616]
13. Eid T, Lee TS, Thomas MJ, Amiry-Moghaddam M, Bjornsen LP, Spencer DD, Agre P, Ottersen OP, de Lanerolle NC. Loss of perivascular aquaporin-4 may underlie deficient water and K^+ homeostasis in the human epileptogenic hippocampus. Proc Natl Acad Sci U S A. 2005; 102:1193–1198. [PubMed: 15657133]
14. Eid T, Thomas MJ, Spencer DD, Runden-Pran E, Lai JC, Malthankar GV, Kim JH, Danbolt NC, Ottersen OP, de Lanerolle NC. Loss of glutamine synthetase in the human epileptogenic hippocampus: possible mechanism for raised extracellular glutamate in mesial temporal lobe epilepsy. Lancet. 2004; 363:28–37. [PubMed: 14723991]
15. Feng Z, Durand DM. Effects of potassium concentration on firing patterns of low-calcium epileptiform activity in anesthetized rat hippocampus: inducing of persistent spike activity. Epilepsia. 2006; 47:727–736. [PubMed: 16650139]
16. Fiacco TA, Agulhon C, Taves SR, Petravicz J, Casper KB, Dong X, Chen J, McCarthy KD. Selective stimulation of astrocyte calcium in situ does not affect neuronal excitatory synaptic activity. Neuron. 2007; 54:611–626. [PubMed: 17521573]
17. Haas CA, Dudeck O, Kirsch M, Huszka C, Kann G, Pollak S, Zentner J, Frotscher M. Role for reelin in the development of granule cell dispersion in temporal lobe epilepsy. J Neurosci. 2002; 22:5797–5802. [PubMed: 12122039]
18. Haas CA, Frotscher M. Reelin deficiency causes granule cell dispersion in epilepsy. Exp Brain Res. 2010; 200:141–149. [PubMed: 19633980]
19. Halassa MM, Haydon PG. Integrated brain circuits: astrocytic networks modulate neuronal activity and behavior. Annu Rev Physiol. 2010; 72:335–355. [PubMed: 20148679]
20. Hammer J, Alvestad S, Osen KK, Skare Ø, Sonnewald U, Ottersen OP. Expression of glutamine synthetase and glutamate dehydrogenase in the latent phase and chronic phase in the kainate model of temporal lobe epilepsy. Glia. 2008; 56:856–868. [PubMed: 18381650]
21. Hinterkeuser S, Schroder W, Hager G, Seifert G, Blumcke I, Elger CE, Schramm J, Steinhäuser C. Astrocytes in the hippocampus of patients with temporal lobe epilepsy display changes in potassium conductances. Eur J Neurosci. 2000; 12:2087–2096. [PubMed: 10886348]
22. Hsu MS, Lee DJ, Binder DK. Potential role of the glial water channel aquaporin-4 in epilepsy. Neuron Glia Biol. 2007; 3:287–297. [PubMed: 18634561]
23. Hsu MS, Seldin M, Lee DJ, Seifert G, Steinhauser C, Binder DK. Laminar-specific and developmental expression of aquaporin-4 in the mouse hippocampus. Neuroscience. 2011; 178:21–32. [PubMed: 21256195]
24. Hugg JW, Butterworth EJ, Kuzniecky RI. Diffusion mapping applied to mesial temporal lobe epilepsy: preliminary observations. Neurology. 1999; 53:173–176. [PubMed: 10408555]
25. Illarionova NB, Gunnarson E, Li Y, Brismar H, Bondar A, Zelenin S, Aperia A. Functional and molecular interactions between aquaporins and Na,K-ATPase. Neuroscience. 2010; 168:915–925. [PubMed: 19962432]
26. Ivens S, Kaufer D, Flores LP, Bechmann I, Zumsteg D, Tomkins O, Seiffert E, Heinemann U, Friedman A. TGF-beta receptor-mediated albumin uptake into astrocytes is involved in neocortical epileptogenesis. Brain. 2007; 130:535–547. [PubMed: 17121744]
27. Jansen LA, Uhlmann EJ, Crino PB, Gutmann DH, Wong M. Epileptogenesis and reduced inward rectifier potassium current in tuberous sclerosis complex-1-deficient astrocytes. Epilepsia. 2005; 46:1871–1880. [PubMed: 16393152]
28. Kang TC, Kim DS, Kwak SE, Kim JE, Won MH, Kim DW, Choi SY, Kwon OS. Epileptogenic roles of astroglial death and regeneration in the dentate gyrus of experimental temporal lobe epilepsy. Glia. 2006; 54:258–271. [PubMed: 16845674]

29. Kivi A, Lehmann TN, Kovacs R, Eilers A, Jauch R, Meencke HJ, von Deimling A, Heinemann U, Gabriel S. Effects of barium on stimulus-induced rises of [K+]o in human epileptic non-sclerotic and sclerotic hippocampal area CA1. Eur J Neurosci. 2000; 12:2039–2048. [PubMed: 10886343]
30. Kofuji P, Ceelen P, Zahs KR, Surbeck LW, Lester HA, Newman EA. Genetic inactivation of an inwardly rectifying potassium channel (Kir4.1 subunit) in mice: phenotypic impact in retina. J Neurosci. 2000; 20:5733–5740. [PubMed: 10908613]
31. Kofuji P, Newman EA. Potassium buffering in the central nervous system. Neuroscience. 2004; 129:1045–1056. [PubMed: 15561419]
32. Lee TS, Eid T, Mane S, Kim JH, Spencer DD, Ottersen OP, de Lanerolle NC. Aquaporin-4 is increased in the sclerotic hippocampus in human temporal lobe epilepsy. Acta Neuropathol. 2004; 108:493–502. [PubMed: 15517312]
33. Ma T, Yang B, Gillespie A, Carlson EJ, Epstein CJ, Verkman AS. Generation and phenotype of a transgenic knockout mouse lacking the mercurial-insensitive water channel aquaporin-4. J Clin Invest. 1997; 100:957–962. [PubMed: 9276712]
34. Manley GT, Binder DK, Papadopoulos MC, Verkman AS. New insights into water transport and edema in the central nervous system from phenotype analysis of aquaporin-4 null mice. Neuroscience. 2004; 129:981–989.
35. Mitchell LA, Jackson GD, Kalnins RM, Saling MM, Fitt GJ, Ashpole RD, Berkovic SF. Anterior temporal abnormality in temporal lobe epilepsy: a quantitative MRI and histopathologic study. Neurology. 1999; 52:327–336. [PubMed: 9932952]
36. Nagelhus EA, Mathiisen TM, Ottersen OP. Aquaporin-4 in the central nervous system: cellular and subcellular distribution and coexpression with Kir4.1. Neuroscience. 2004; 129:905–913. [PubMed: 15561407]
37. Neusch C, Papadopoulos N, Muller M, Maletzki I, Winter SM, Hirrlinger J, Handschuh M, Bahr M, Richter DW, Kirchhoff F, Hulsmann S. Lack of the Kir4.1 channel subunit abolishes K+ buffering properties of astrocytes in the ventral respiratory group: impact on extracellular K+ regulation. J Neurophysiol. 2006; 95:1843–1852. [PubMed: 16306174]
38. Newman EA. High potassium conductance in astrocyte endfeet. Science. 1986; 233:453–454. [PubMed: 3726539]
39. Newman EA, Frambach DA, Odette LL. Control of extracellular potassium levels by retinal glial cell K^+ siphoning. Science. 1984; 225:1174–1175. [PubMed: 6474173]
40. Nielsen S, Nagelhus EA, Amiry-Moghaddam M, Bourque C, Agre P, Ottersen OP. Specialized membrane domains for water transport in glial cells: high-resolution immunogold cytochemistry of aquaporin-4 in rat brain. J Neurosci. 1997; 17:171–180. [PubMed: 8987746]
41. Nitta N, Heinrich C, Hirai H, Suzuki F. Granule cell dispersion develops without neurogenesis and does not fully depend on astroglial cell generation in a mouse model of temporal lobe epilepsy. Epilepsia. 2008; 49:1711–1722. [PubMed: 18397295]
42. Pallud J, Haussler U, Langlois M, Hamelin S, Devaux B, Deransart C, Depaulis A. Dentate gyrus and hilus transection blocks seizure propagation and granule cell dispersion in a mouse model for mesial temporal lobe epilepsy. Hippocampus. 2010
43. Paxinos, G.; Franklin, KBJ. The mouse brain in stereotaxic coordinates. Academic Press; San Diego: 2001.
44. Poopalasundaram S, Knott C, Shamotienko OG, Foran PG, Dolly JO, Ghiani CA, Gallo V, Wilkin GP. Glial heterogeneity in expression of the inwardly rectifying K(+) channel, Kir4.1, in adult rat CNS. Glia. 2000; 30:362–372. [PubMed: 10797616]
45. Riban V, Bouilleret V, Pham-Le BT, Fritschy JM, Marescaux C, Depaulis A. Evolution of hippocampal epileptic activity during the development of hippocampal sclerosis in a mouse model of temporal lobe epilepsy. Neuroscience. 2002; 112:101–111. [PubMed: 12044475]
46. Roper SN, Obenhaus A, Dudek FE. Osmolality and nonsynaptic epileptiform bursts in rat CA1 and dentate gyrus. Ann Neurol. 1992; 31:81–85. [PubMed: 1543352]
47. Saadoun S, Papadopoulos MC, Watanabe H, Yan D, Manley GT, Verkman AS. Involvement of aquaporin-4 in astroglial cell migration and glial scar formation. J Cell Sci. 2005; 118:5691–5698. [PubMed: 16303850]

48. Schmued LC, Albertson C, Slikker W. Fluoro-Jade: a novel fluorochrome for the sensitive and reliable histochemical localization of neuronal degeneration. Brain Research. 1997; 751:37–46. [PubMed: 9098566]
49. Schwartzkroin PA, Baraban SC, Hochman DW. Osmolarity, ionic flux, and changes in brain excitability. Epilepsy Res. 1998; 32:275–285. [PubMed: 9761327]
50. Seifert G, Huttmann K, Binder DK, Hartmann C, Wyczynski A, Neusch C, Steinhäuser C. Analysis of astroglial K+ channel expression in the developing hippocampus reveals a predominant role of the Kir4.1 subunit. J Neurosci. 2009; 29:7474–7488. [PubMed: 19515915]
51. Seifert G, Schilling K, Steinhäuser C. Astrocyte dysfunction in neurological disorders: a molecular perspective. Nat Rev Neurosci. 2006; 7:194–206. [PubMed: 16495941]
52. Steinhäuser C, Seifert G. Glial membrane channels and receptors in epilepsy: impact for generation and spread of seizure activity. European Journal of Pharmacology. 2002; 447:227–237. [PubMed: 12151014]
53. Stewart TH, Eastman CL, Groblewski PA, Fender JS, Verley DR, Cook DG, D'Ambrosio R. Chronic dysfunction of astrocytic inwardly rectifying K+ channels specific to the neocortical epileptic focus after fluid percussion injury in the rat. J Neurophysiol. 2010
54. Takahashi DK, Vargas JR, Wilcox KS. Increased coupling and altered glutamate transport currents in astrocytes following kainic-acid-induced status epilepticus. Neurobiol Dis. 2010; 40:573–585. [PubMed: 20691786]
55. Tian GF, Azmi H, Takano T, Xu Q, Peng W, Lin J, Oberheim N, Lou N, Wang X, Zielke HR, Kang J, Nedergaard M. An astrocytic basis of epilepsy. Nature Medicine. 2005; 11:973–981.
56. Traynelis SF, Dingledine R. Potassium-induced spontaneous electrographic seizures in the rat hippocampal slice. J Neurophysiol. 1988; 59:259–276. [PubMed: 3343603]
57. Traynelis SF, Dingledine R. Role of extracellular space in hyperosmotic suppression of potassium-induced electrographic seizures. J Neurophysiol. 1989; 61:927–938. [PubMed: 2723735]
58. Vajda Z, Pedersen M, Fuchtbauer EM, Wertz K, Stodkilde-Jorgensen H, Sulyok E, Doczi T, Neely JD, Agre P, Frokiaer J, Nielsen S. Delayed onset of brain edema and mislocalization of aquaporin-4 in dystrophin-null transgenic mice. Proc. Natl. Acad. Sci. USA. 2002; 99:13131–13136.
59. van der Hel WS, Notenboom RGE, Bos IWM, van Rijen PC, van Veelen CWM, de Graan PNE. Reduced glutamine synthetase in hippocampal areas with neuron loss in temporal lobe epilepsy. Neurology. 2005; 64:326–333. [PubMed: 15668432]
60. Verkman AS. Physiological importance of aquaporin water channels. Ann Med. 2002; 34:192–200. [PubMed: 12173689]
61. Verkman AS. More than just water channels: unexpected cellular roles of aquaporins. J Cell Sci. 2005; 118:3225–3232. [PubMed: 16079275]
62. Vezzani A, Granata T. Brain inflammation in epilepsy: experimental and clinical evidence. Epilepsia. 2005; 46:1724–1743. [PubMed: 16302852]
63. Volterra A, Meldolesi J. Astrocytes, from brain glue to communication elements: the revolution continues. Nat Rev Neurosci. 2005; 6:626–640. [PubMed: 16025096]
64. Wetherington J, Serrano G, Dingledine R. Astrocytes in the epileptic brain. Neuron. 2008; 58:168–178. [PubMed: 18439402]
65. Wolburg-Buchholz K, Mack A, Steiner E, Pfeiffer F, Engelhardt B, Wolburg H. Loss of astrocyte polarity marks blood-brain barrier impairment during experimental autoimmune encephalomyelitis. Acta Neuropathol. 2009; 118:219–233. [PubMed: 19533155]
66. Zhang H, Verkman AS. Aquaporin-4 independent Kir4.1 K+ channel function in brain glial cells. Molecular and Cellular Neuroscience. 2008; 37:1–10. [PubMed: 17869537]

HIGHLIGHTS

- AQP4-deficient mice had more spontaneous recurrent seizures than wild-type mice
- Prolonged downregulation of AQP4 was observed in the hippocampus following seizures
- $AQP4^{-/-}$ mice had increased fluoro-jade positive cells early after seizures
- Intense seizures may lead to a dysregulation of water and K^+ homeostasis

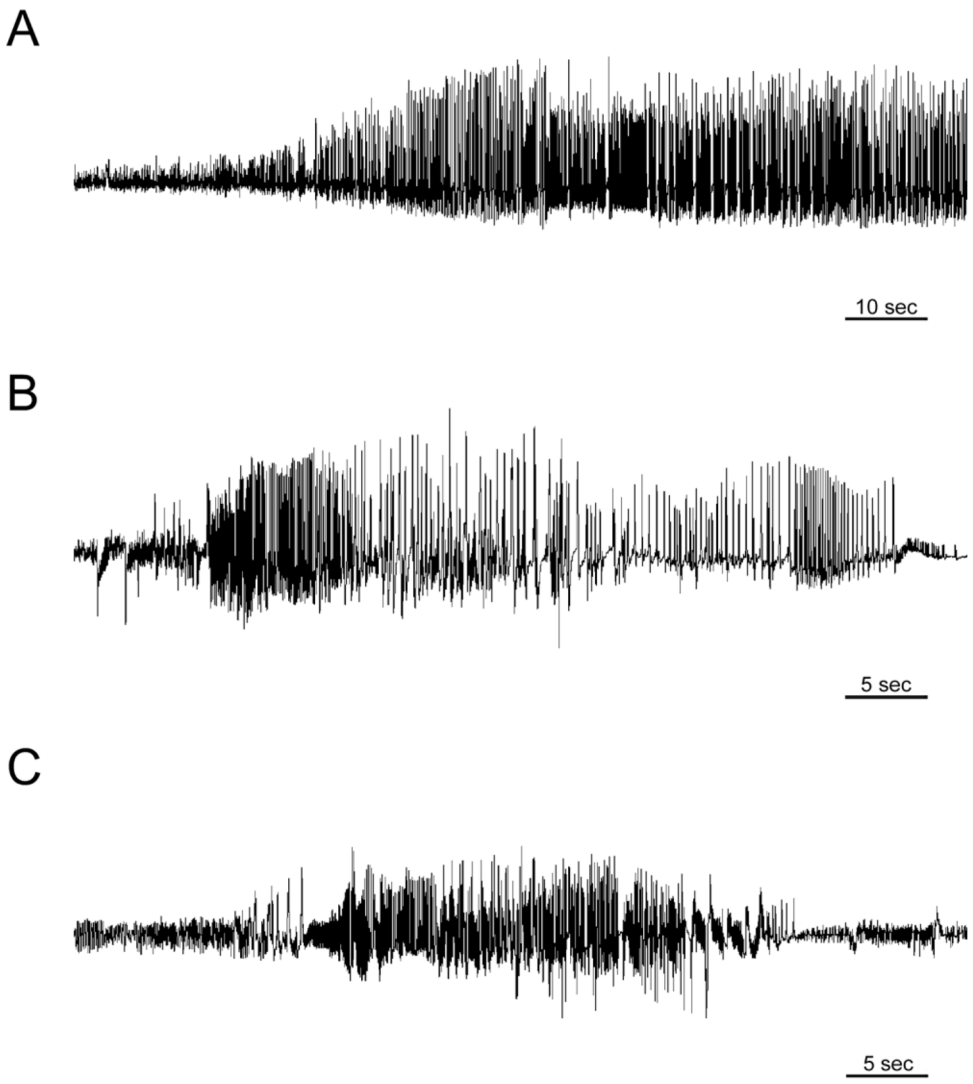

Figure 1.

Intrahippocampal kainic acid model. A. EEG recording during status epilepticus. Within the first 30 minutes after kainic acid injection, the mouse develops electrographic and behavioral status epilepticus. B. Example of EEG recording of a spontaneous seizure in an $AQP4^{+/+}$ mouse. C. Example of EEG recording of a spontaneous seizure in an $AQP4^{-/-}$ mice. Within 2–7 days post-injection, both $AQP4^{+/+}$ and $AQP4^{-/-}$ mice which underwent status epilepticus developed spontaneous seizures.

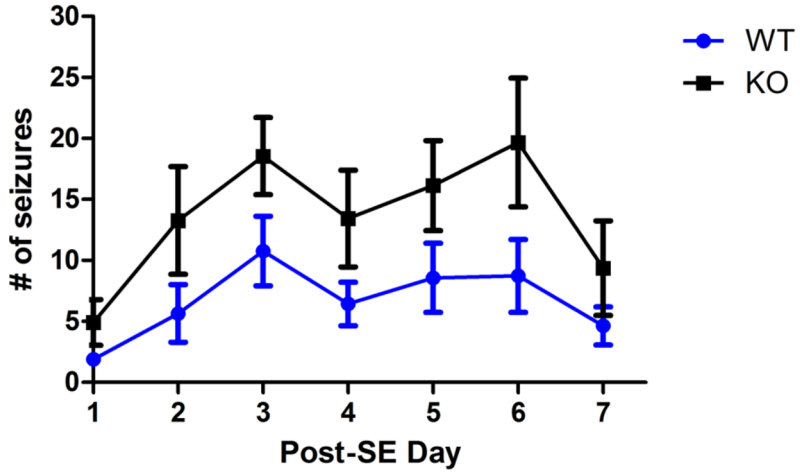

Figure 2.

Increased seizure frequency in AQP4$^{-/-}$ mice. Both AQP4$^{+/+}$ and AQP4$^{-/-}$ mice developed spontaneous seizures after undergoing status epilepticus; however, AQP4$^{-/-}$ mice exhibited more seizures during the epileptogenic period (post-status epilepticus days 1–7, 2-way RM ANOVA, $p<0.05$).

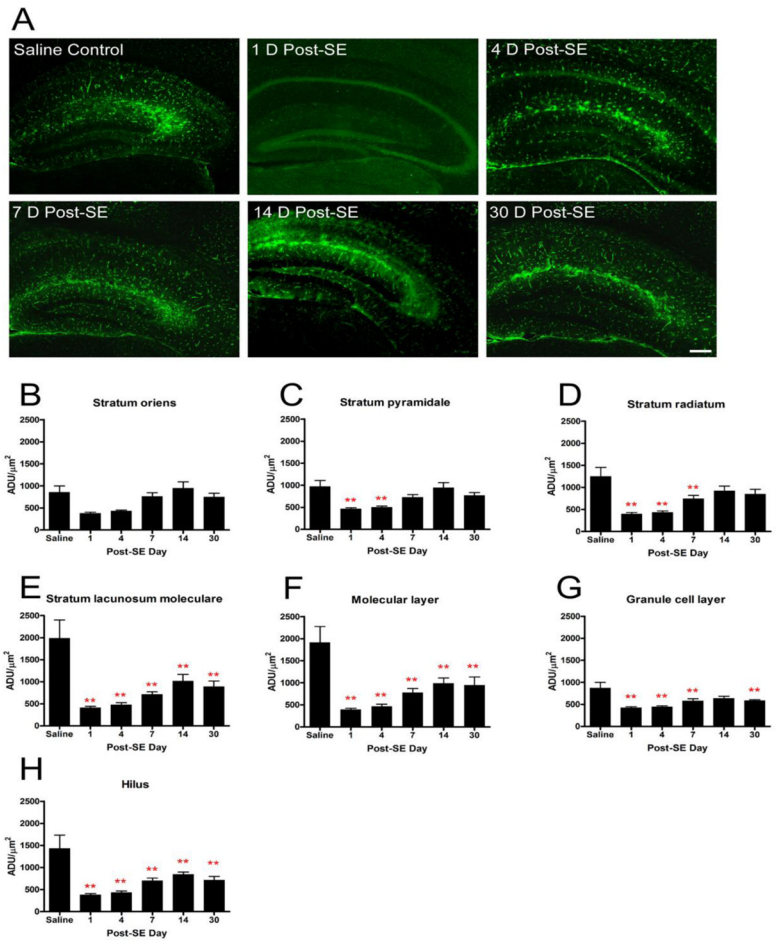

Figure 3.

AQP4 immunoreactivity following kainic acid status epilepticus. Significant reduction in hippocampal AQP4 immunoreactivity was observed with delayed partial recovery. A. 4x images at indicated time points after SE. Scale bar = 200 μm. Laminar-specific analysis of AQP4 immunoreactivity after SE demonstrates decreased AQP4 immunoreactivity detected in various layers of the hippocampus throughout the study period (B-H). The initial decrease in AQP4 immunoreactivity is followed by a gradual increase. Persistent downregulation was observed in the SLM, ML, granule cell layer and hilus. ADU= arbitrary density units. **, $p<0.01$ compared to saline control.

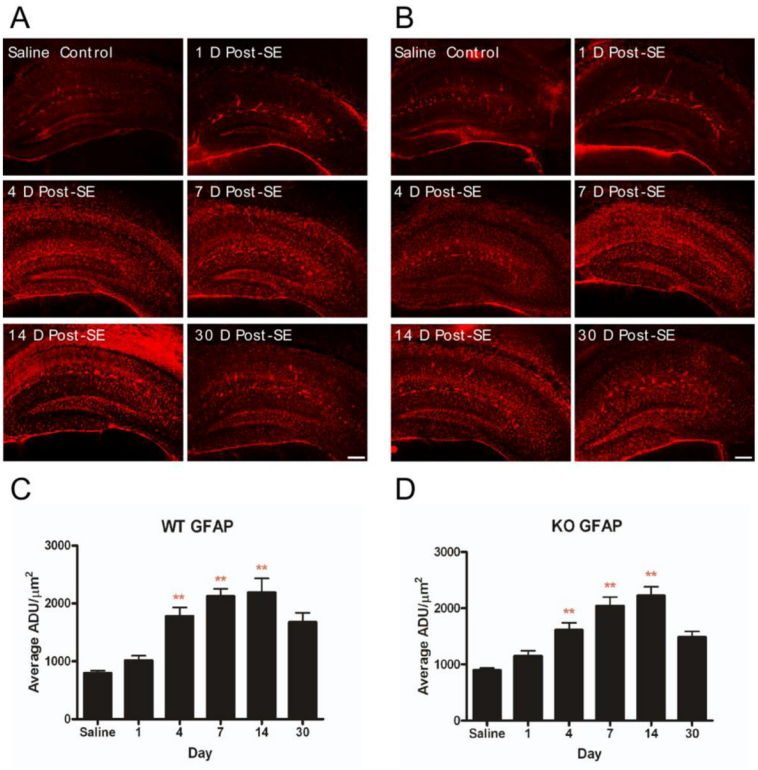

Figure 4.

Immunohistochemical staining of GFAP. Increased GFAP immunoreactivity and astrocyte ramification occurs following SE in both $AQP4^{+/+}$ (A, C) and $AQP4^{-/-}$ (B, D) mice. Scale bar = 200 μm.

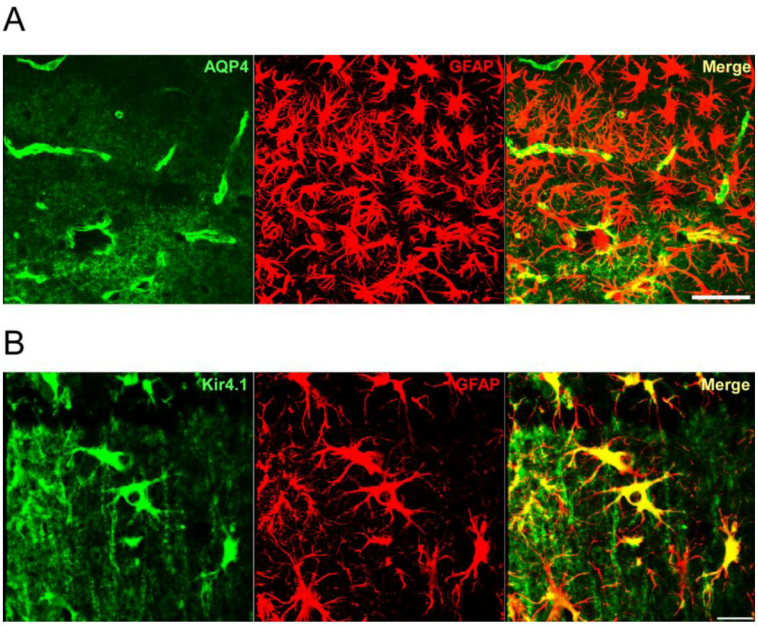

Figure 5.

Comparison of AQP4 and $K_{ir}4.1$ labeling of reactive astrocytes. A. Confocal 40x image in CA1 stratum lacunosum moleculare 7 days post-SE. Note marked reactive phenotype of GFAP-positive astrocytes (center) but lack of strong AQP4 immunoreactivity. Scale bar = 50μm. B. Confocal 63x image of reactive astrocytes in CA1 stratum radiatum 14 days post-SE. Note strong $K_{ir}4.1$ immunoreactivity on reactive astrocytes. Scale bar = 20μm.

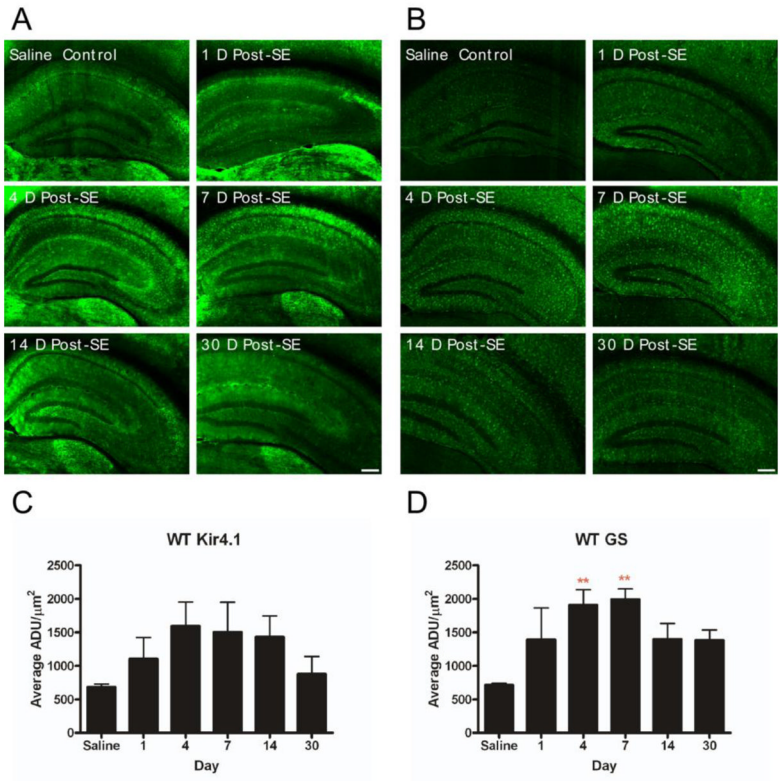

Figure 6.

K_{ir}4.1 and glutamine synthetase immunoreactivity. A, C. No significant overall change in K_{ir}4.1 immunoreactivity was observed post-SE. However, focal increase in K_{ir}4.1 immunoreactivity was detected within the ramified astrocytes of the stratum radiatum and stratum lacunosum moleculare during post-SE days 4 and 7 (Supplemental Figure 2). B, D. Glutamine synthetase immunoreactivity was transiently elevated at post-SE days 4 and 7. Scale bar = 200μm.

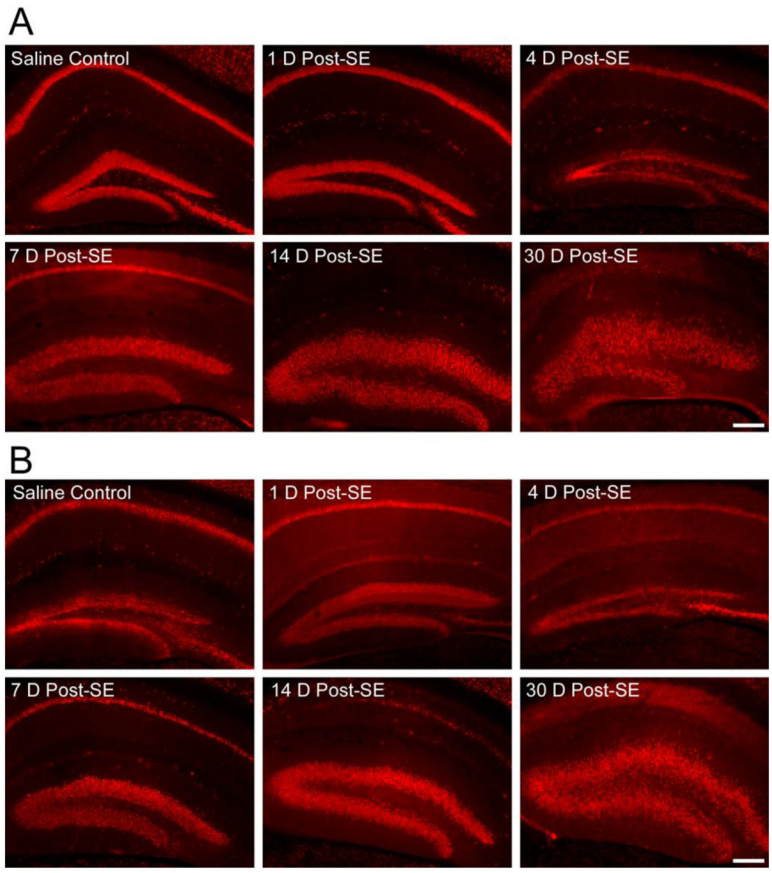

Figure 7.

Granule cell dispersion and CA1 pyramidal cell loss following intrahippocampal KA administration. After KA-induced SE, granule cell dispersion was noted in both $AQP4^{+/+}$ (A) and $AQP4^{-/-}$ (B) mice as early as post-SE day 7. Granule cell dispersion was observed at post-SE day 14 and 30, and is accompanied by loss of NeuN immunoreactivity in the CA1 pyramidal cell layer. Scale bar = 200μm.

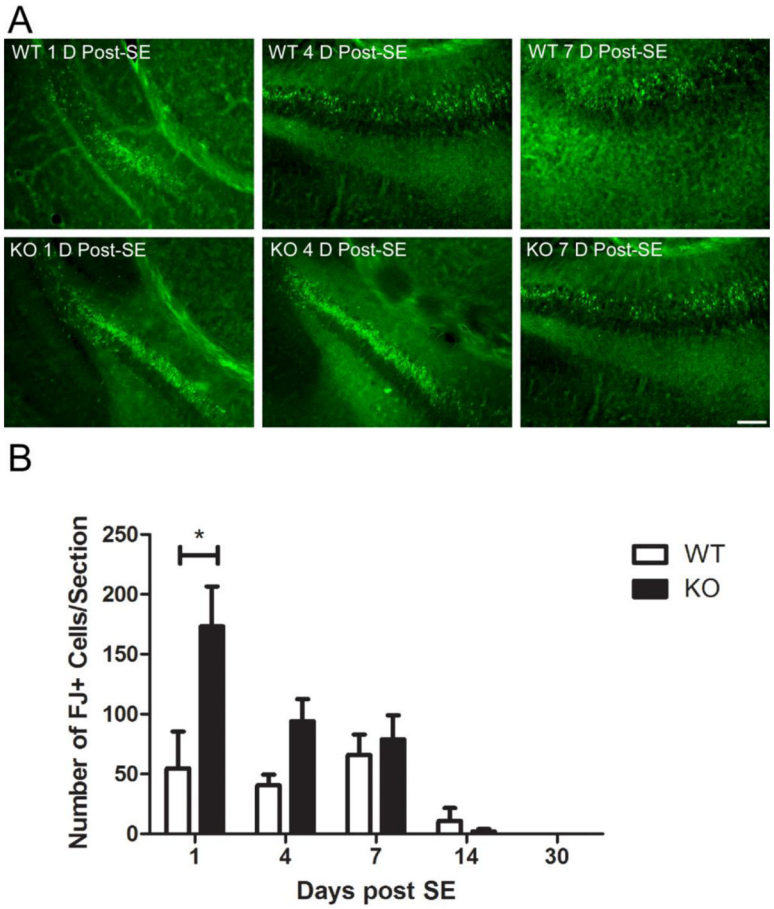

Figure 8.

Fluoro-jade-B histochemistry following SE. A. Representative examples of FJ-B-positive cells in the CA3 region and hilus of the dentate gyrus in the hippocampus ipsilateral to the injection in AQP4$^{+/+}$ and AQP4$^{-/-}$ mice. Scale bar = 100μm. B. There were significantly more FJ-B-positive cells within AQP4$^{-/-}$ hippocampi relative to AQP4$^{+/+}$ hippocampi on post-SE day 1 (2-way ANOVA with post-hoc Bonferroni test, $P<0.001$).